SZC010 suppresses breast cancer development by regulating the PI3K/Akt/NF-κB signaling pathway

Junhan Jiang[1], Xiaorui Li[2], Hongtao Xu[3], Yiwen Ma[2], Meiyi Fu[2], Xiangyu Guo[2], Tao Sun[2], Xinyu Zheng[1,4]

[1]Department of Breast Surgery, the First Hospital of China Medical University, Shenyang, China; [2]Department of Breast Oncology, Cancer Hospital of China Medical University, Liaoning Cancer Hospital, Shenyang, China; [3]ICU Department, Cancer Hospital of China Medical University, Liaoning Cancer Hospital, Shenyang, China; [4]Lab 1, Cancer Institute, the First Hospital of China Medical University, Shenyang, China

Contributions: (I) Conception and design: T Sun, X Zheng; (II) Administrative support: X Zheng; (III) Provision of study materials or patients: J Jiang, X Li; (IV) Collection and assembly of data: H Xu, X Guo; (V) Data analysis and interpretation: M Fu; (VI) Manuscript writing: All authors; (VII) Final approval of manuscript: All authors.

Correspondence to: Dr. Xinyu Zheng, MD. Department of Breast Surgery, the First Hospital of China Medical University, Shenyang 110001, China; Lab 1, Cancer Institute, the First Hospital of China Medical University, No. 155 Nanjing North Street, Heping District, Shenyang 110001, China. Email: xyzheng@cmu.edu.cn.

Background: Breast cancer has become one of the leading causes of cancer deaths and is the most frequently diagnosed cancer among females worldwide. Despite advances in breast cancer therapy, metastatic disease in most patients will eventually progress due to the development of *de novo* or secondary resistance. Thus, it is extremely important to seek novel drugs with high effectiveness and low toxicity for systematic therapy.

Methods: We applied a 3-(4,5-Dimethylthiazol-2-yl)-2,5-diphenyltetrazolium bromide (MTT) assay in this study to analyze and evaluate the cytotoxic activity of oleanolic acid (OA) and its derivatives in three types of breast cancer cell lines (MDA-MB-231, MCF-7, and MDA-MB-453). A flow cytometry assay was performed to access the mechanisms of apoptosis and cell cycle analysis in SZC010 in MDA-MB-453 cells. Apoptosis- and cyclin-related proteins were evaluated by western blot. The key proteins of the NF-κB and PI3K-Akt-mTOR signaling pathway were also evaluated by western blot.

Results: Our results revealed that all OA derivatives were more effective than OA in three types of breast cancer cell lines (MCF-7, MDA-MB-231, and MDA-MB-453). Among these seven OA derivatives, SZC010 exhibited the most potent cytotoxicity in MDA-MB-453 cells. Additionally, we observed that SZC010 treatment induced dose-and time-dependent growth inhibition in MDA-MB-453 cells. Furthermore, we demonstrated that SZC010 induced growth arrest in the G2/M phase and apoptosis by inhibition of NF-κB activation via the PI3K/Akt/mTOR signaling pathway.

Conclusions: Our data indicate that the novel OA derivative, SZC010, has great potential in breast cancer therapy.

Keywords: Oleanolic acid (OA); apoptosis; NF-κB; PI3K/Akt/mTOR signaling pathway; breast cancer cells

Submitted Jan 23, 2024. Accepted for publication Jun 24, 2024. Published online Jun 28, 2024.
doi: 10.21037/cco-24-10
View this article at: https://dx.doi.org/10.21037/cco-24-10

Introduction

According to the 2022 Global Cancer Statistics, breast cancer is now the most frequently diagnosed cancer among women worldwide and one of the leading causes of cancer-related mortality (1,2). Over recent decades, conventional therapies (including surgery, chemotherapy, radiotherapy, endocrine therapy, and targeted therapy) have significantly reduced the risk of disease recurrence and death in breast

© Chinese Clinical Oncology. All rights reserved.

cancer patients (3-10). Despite continuous improvements in oncologic outcomes, most patients with advanced breast cancer ultimately succumb to their disease due to therapy resistance (11,12). Therefore, it is extremely important to identify efficient and safe drugs to treat breast cancer.

Phytochemicals with antioxidant, anti-inflammatory, and immunomodulatory activities are commonly used as alternative or complementary therapies for cancer (13,14). Oleanolic acid (OA), a prevalent phytochemical, occurs in nature as a free acid or as an aglycone of triterpenoid saponins (15). OA exhibits antitumor activity against numerous neoplasms, including hepatocellular cancer (16), hematological malignancies (17), lung cancer (18), ovarian cancer (19), pancreatic cancer (20), skin cancer (21), and glioblastoma (22). Despite its effectiveness, research and clinical applications of OA are limited due to its poor water solubility (23). The potential mechanisms underlying the anti-breast cancer activities of OA and its derivatives have not yet been elucidated. In the present study, seven derivatives of OA were synthesized, and their anti-cancer activities were examined in three breast cancer cell lines (MCF-7, MDA-MB-231, and MDA-MB-453). In addition, the underlying molecular mechanisms of its anti-cancer activity were explored. Our findings indicated that all OA derivatives were more effective than OA itself in breast cancer cells and the fused heterocycle derivative SZC010 could be a promising drug for the suppression of breast cancer. We present this article in accordance with the MDAR and ARRIVE reporting checklists (available at https://cco.amegroups.com/article/view/10.21037/cco-24-10/rc).

Highlight box

Key findings

- Oleanolic acid (OA) derivatives were more effective than OA in breast cancer cell lines.
- SZC010 has great potential in breast cancer therapy.
- SZC010 regulates the PI3K/Akt/NF-κB signaling pathway.

What is known and what is new?

- The anti-cancer potential of OA derivatives is well-established.
- We found that the OA derivative, SZC010, has great potential in breast cancer therapy by regulating the PI3K/Akt/NF-κB signaling pathway.

What are the implications, and what should change now?

- SZC010 may be a potential anti-tumor agent in breast cancer, which needs to be verified by clinical trials.

Methods

Synthesis of OA derivatives

OA derivatives, SZC009, SZC010, SZC012, SZC013, SZC014, SZC015, and SZC017, were synthesized by Professor Shisheng Wang from the Dalian University of Technology (*Figure 1*).

Cell culture

We performed our cell culture experiments using the following breast cancer cell lines: MCF-7, MDA-MB-231, and MDA-MB-453 cells. The human breast cancer MCF-7, MDA-MB-231, and MDA-MB-453 cell lines were cultivated at 37 ℃ with 5% CO_2. MCF-7 cells were cultivated in minimum essential medium (41500-034; Thermo Fisher Scientific, Inc., China) with 10% fetal bovine serum (FBS; 10439024; Thermo Fisher Scientific, Inc.), 1% non-essential amino acids (11140050), and 1 mM sodium pyruvate (11360070; Thermo Fisher Scientific, Inc.). MDA-MB-231 and MDA-MB-453 cells were cultivated in Dulbecco's modified Eagle's medium (DMEM; 12800-058; Thermo Fisher Scientific, Inc.) with 10% FBS (10439024; Thermo Fisher Scientific, Inc.). The cells were seeded in six-well plates or other appropriate dishes (30,000 cells/mL).

Cell viability assay

The 3-(4,5-Dimethyl-2-thiazolyl)-2,5-diphenyl-2H-tetrazolium bromide (MTT) assay was used to assess cell viability. Breast cancer MCF-7, MDA-MB-231, and MDA-MB-453 cells were cultured in 96-well plates at a density of 1×10^5 cells/well, and then treated with 0, 10, 20, 40, and 80 μmol/L OA and OA derivatives (SZC009, SZC010, SZC012, SZC013, SZC014, SZC015, and SZC017) for 24 h. Furthermore, MDA-MB-453 and MCF-10A cells were treated with 0, 5, 10, 15, 20, 30, and 40 μmol/L SZC010 for 0, 12, 24, 48, and 72 h. Dimethyl sulfoxide at the same dilution was used as the control. Following treatment, MTT was added in each well (5 mg/mL) and incubated at 37 ℃ for 2 h. Formazan crystals were dissolved in 100 μL Triple solution and absorbance was measured using a microplate reader (Multiskan MK3; Pioneer Co-operative UK Ltd., Hong Kong, China). Each experiment was performed at least in quintuplicate. The cytotoxic effects of OA and its derivatives are expressed as IC50 values, which were calculated using the Probit model of IBM SPSS Statistics 19.

© Chinese Clinical Oncology. All rights reserved.

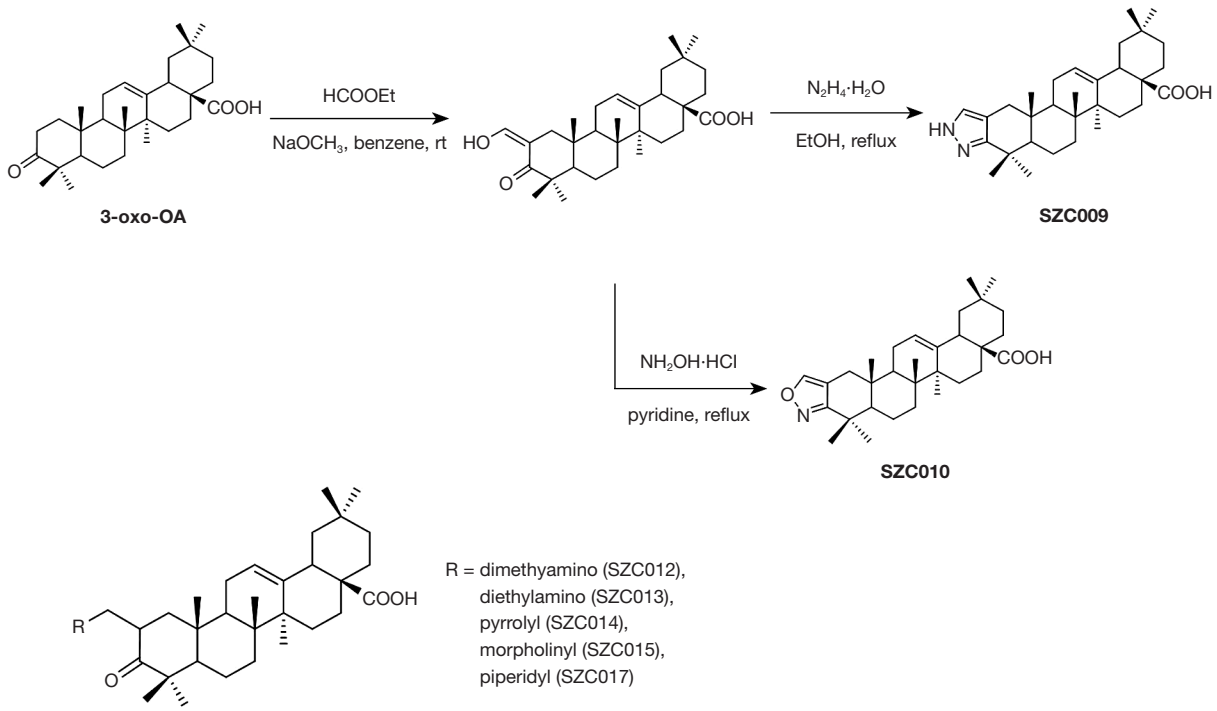

Figure 1 Synthesis of the fused heterocycle (SZC009 and SZC010) and Mannich base (SZC012, SZC013, SZC014, SZC015, and SZC017) derivatives.

Apoptosis analysis

Apoptosis was detected using annexin V fluorescein isothiocyanate (FITC)/propidium iodide (PI) staining according to the manufacturer's instructions. MDA-MB-453 cells were seeded in six-well plates (1×10^6 cells/well) and incubated with 15 μmol/L SZC010 for 0, 12, 24, and 48 h. Following incubation, the cells were collected and incubated at room temperature with 5 μL of Annexin-V/FITC (C1052; Beyotime Institute of Biotechnology, China) in binding buffer in the dark for 20 min. PI solution was then added for an additional 10-min incubation. The cells were analyzed by fluorescence-activated cell sorting (FACS) using a flow cytometer (BD FACSAria II; BD Co., New Jersey, USA).

Cell cycle analysis

The cell cycle was assessed using PI staining according to the manufacturer's instructions. MDA-MB-453 cells cultured in six-well plates (1×10^6 cells/well) were synchronized by serum starvation overnight and incubated with 15 μmol/L SZC010 for 0, 12, 24, and 48 h. Following incubation, the cells were fixed with 70% ethanol at 4 ℃ overnight and resuspended in ice-cold phosphate-buffered saline (PBS). Next, a cell cycle solution (C1052; Beyotime Institute of Biotechnology) containing 20 μg/mL RNase A and 50 μg/mL PI was used to incubate the cells in the dark for 30 min. A flow cytometer (BD FACSAria II; BD Co.) was then used to determine the cell cycle distribution of the cells.

Cell morphology and ultrastructure observation

MDA-MB-453 cells were seeded in six-well plates (1×10^6 cells/well) and incubated with 15 μmol/L SZC010 for 0, 12, 24, and 48 h. Following incubation, an inverted phase contrast microscope (LV-150N; Nikon Corporation; Japan) was used to observe changes in cell morphology. Furthermore, the cells were collected by centrifugation and fixed with 2.5% glutaraldehyde at 4 ℃ overnight. Next, the cells were post-fixed in osmium tetraoxide for 30 min, dehydrated in ethanol, embedded in Epon 812 resin, and stained with lead citrate and uranyl acetate. Finally, a transmission electron microscope (JEM-2000EX;

© Chinese Clinical Oncology. All rights reserved.

JEOL, Ltd., Tokyo, Japan) was used to observe the cell ultrastructure changes.

Western blotting analysis

MDA-MB-453 cells were cultured in six-well plates (1×10^6 cells/well) and incubated with 15 μmol/L SZC010 for 0, 12, 24, and 48 h. A Nuclear and Cytoplasmic Extraction Reagents kit (Thermo Fisher Scientific, Inc.; 78835) was used to collect the nuclear and cytoplasmic fractions. The cytoplasmic and nuclear protein extracts were reconstituted in a loading buffer (Beyotime Institute of Biotechnology) and boiled for 5 min. Equal amounts of protein (30 μg/sample) were separated by electrophoresis in 12% Sodium Dodecyl Sulfate PolyAcrylamide Gel Electrophoresis (SDS-PAGE) and transferred onto polyvinylidene fluoride (PVDF) membranes. After blocking with 5% dried non-fat milk in tris-buffered saline (TBS) containing 0.05% Tween 20 for 1 h at 25 ℃, the membranes were incubated with the primary antibody (Abcam; the US) at 4 ℃ overnight and washed with TBS for 5 min. Subsequently, they were incubated with horseradish peroxidase-conjugated secondary antibodies for 2 h at 25 ℃. The blots were developed by chemiluminescence and detected using an ImageQuant Analyzer (ImageQuant LAS 4000, GE Healthcare; the US). The optical density of protein blots was quantified using Quantity One software.

Xenograft model

Healthy female nude mice (5–6 weeks old) were purchased from Beijing HFK Bioscience Co., Ltd. and maintained under pathogen-free conditions. To establish breast cancer xenografts, MDA-MB-453 tumor cells (1×10^7) were injected into the armpits of the mice. One week after implantation, the mice were randomized into vehicle (n=8) and treated (10 mg/kg SZC010) groups. SZC010, dissolved in 5% dimethyl sulfoxide (DMSO) and 10% Tween-20 in PBS, was administered intraperitoneally once every two days for two consecutive weeks. The control group received the vehicle only. Tumor volume was measured twice a week and calculated using the formula: (length × width × depth ×0.52), and body weights were recorded daily. After the mice were sacrificed, the xenograft tumors were removed and either frozen in liquid nitrogen or fixed in 4% formalin and embedded in paraffin for further studies. Animal experiments were performed under a project license (No. CMU2023040) granted by Animal Ethics Committee board of China Medical University, in compliance with China Medical University's guidelines for the care and use of animals. A protocol was prepared before the study without registration.

Statistical analysis

Data from at least three independent experiments are presented as the mean ± standard error. One-way analysis of variance (ANOVA) was used for statistical analysis, followed by the Student's *t*-test to compare two groups. All statistical analyses were performed using SPSS 19.0 for Windows and GraphPad Prism version 8.02. A P value of less than 0.05 was considered statistically significant.

Results

OA derivatives significantly suppress breast cancer cell growth

To evaluate the anti-breast cancer effect of OA and its derivatives, MCF-7 (luminal type), MDA-MB-231 (triple-negative type), and MDA-MB-453 (HER2-positive type) cells were tested following the application of increasing concentrations (0, 5, 10, 20, 40, and 80 μmol/L) of compounds for 24 h and analyzed using an MTT assay. The analysis showed that OA and its derivatives exhibited cytotoxic activity against MCF-7, MDA-MB-231, and MDA-MB-453 cells (*Figure 2A*).

OA (5–40 μmol/L) treatment for 24 h did not have any effect on the cell proliferation of MCF-7, MDA-MB-231, and MDA-MB-453 cell lines compared to the untreated cells (IC_{50} values: 94.01, 122.76, and 119.07 μmol/L, respectively). All OA derivatives were more effective than OA (IC_{50} values: 17.14–92.53 μmol/L). Treatment with SZC012 and SZC014 for 24 h significantly inhibited MCF-7 cells, as compared to other derivatives (IC_{50} values: 22.95 and 26.07 μmol/L, respectively). Also, treatment with SZC014 for 24 h significantly inhibited MDA-MB-231 cells, with an IC_{50} value of 23.23 μmol/L. Treatment with SZC009 and SZC010 for 24 h significantly inhibited MDA-MB-453 cells (IC_{50} values: 27.79 and 17.14 μmol/L, respectively).

In general, all OA derivatives were more effective than OA in three types of breast cancer cell lines (MCF-7, MDA-MB-231, and MDA-MB-453). Among these nitrogen-containing OA derivatives, Mannich base derivatives exhibited a superior anti-proliferative activity than that by fused heterocycle derivatives in MCF-7 and MDA-MB-231 cell lines, while the fused heterocycle derivatives were more

© Chinese Clinical Oncology. All rights reserved.

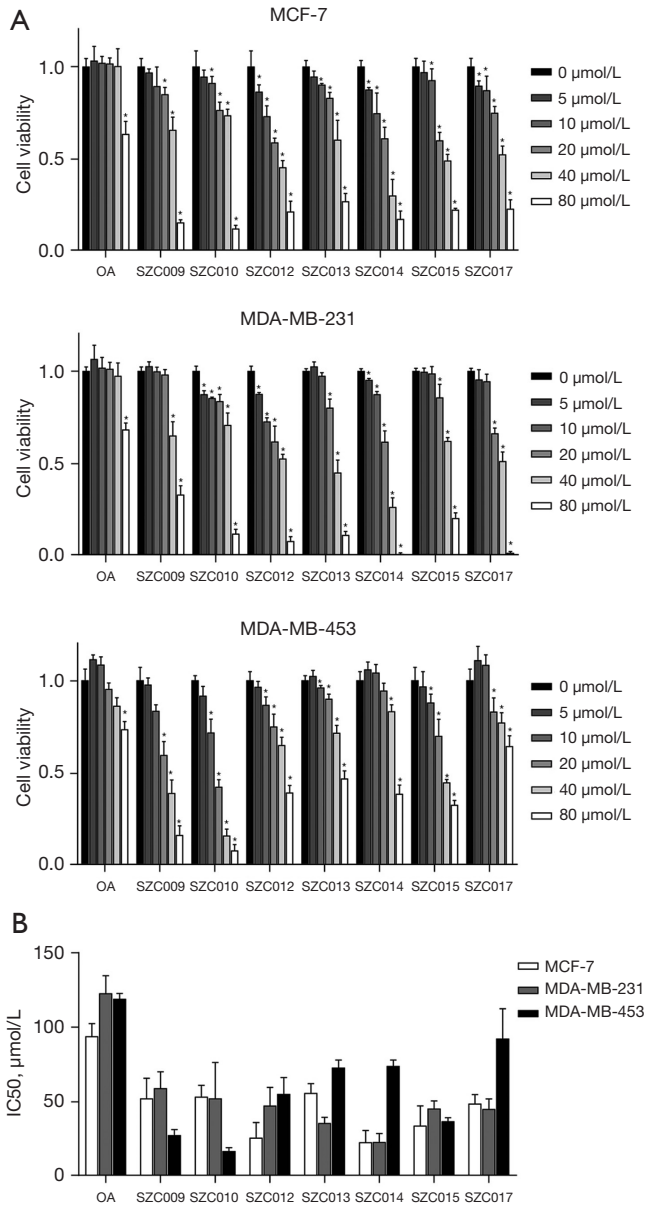

Figure 2 Cytotoxicity of OA and its derivatives in the MCF-7, MDA-MB-231, and MDA-MB-453 cell lines. MCF-7, MDA-MB-231, and MDA-MB-453 cells were treated with OA and its derivatives (0–80 μmol/L) for 24 h. (A) Histogram showing the percentage of viable cells following treatment with 0, 5, 10, 20, 40, and 80 μmol/L of OA and its derivatives for 24 h, as determined by the MTT assay. Data are expressed as the mean ± SEM of three independent experiments performed in triplicate (n=3; *, P<0.05). (B) Histogram showing the IC50 values (24 h) of OA and its derivatives in the MCF-7, MDA-MB-231, and MDA-MB-453 cells. OA, oleanolic acid; MTT, 3-(4,5-Dimethyl-2-thiazolyl)-2,5-diphenyl-2H-tetrazolium bromide; SEM, standard error of the mean.

effective in MDA-MB-453 cell lines. Moreover, treatment with the fused heterocycle derivative SZC010 significantly inhibited MDA-MB-453 cell lines, as compared to other derivatives, with an IC50 value at 17.14 μmol/L, which indicated that SZC010 is a more potent anti-proliferative agent for MDA-MB-453 breast cancer (*Figure 2B*).

SZC010 inhibits MDA-MB-453 cells in a dose- and time-dependent manner

To further evaluate the anti-MDA-MB-453 cell effect of SZC010, the MDA-MB-453 cell line was treated with various concentrations of SZC010 (5, 10, 20, 30, and 40 μmol/L) for various time periods (12, 24, 48, and 72 h). The growth inhibition of the MDA-MB-453 cell line was found to be dose- and time-dependent following SZC010 treatment (*Figure 3A*). The IC50 value of SZC010 was 21.60 μmol/L at 12 h, 16.79 μmol/L at 24 h, 12.14 μmol/L at 48 h, and 10.08 μmol/L at 72 h. By contrast, the cytotoxicity of SZC010 in the mammary epithelial MCF-10A cell line was also evaluated. The results revealed that SZC010 (0–40 μmol/L) did not have an effect on MCF-10A cell proliferation (*Figure 3B*). These findings suggested that SZC010 was a selective anti-cancer agent against MDA-MB-453 breast cancer cells.

SZC010 induces apoptosis in MDA-MB-453 cells

Light and transmission electron microscopes were used to observe the SZC010-dependent changes in cell morphology and ultrastructure. The results demonstrated the occurrence of cell shrinkage, microvilli absence, chromatin condensation, nuclei fragmentation, and apoptosis bodies following treatment with SZC010 (*Figure 4A*). Flow cytometry was performed with annexin V FITC/PI double staining to determine whether apoptosis contributed to the inhibition of MDA-MB-453 cell growth induced by SZC010. As shown in *Figure 4B*, the apoptosis percentages of SZC010 (15 μmol/L) in the 12, 24, and 48 h groups were 5.49%±1.98%, 12.28%±1.05%, and 17.71%±0.63%, respectively, which was significantly higher than that in the control group (1.28%±0.09%).

SZC010 induces caspase-dependent apoptosis through intrinsic pathways

To further explore the molecular mechanism of SZC010-induced MDA-MB-453 cell apoptosis, western blotting

© Chinese Clinical Oncology. All rights reserved.

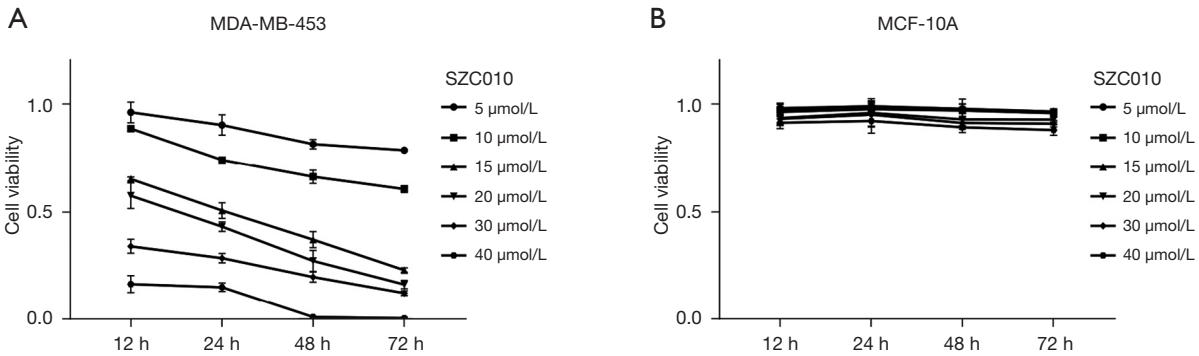

Figure 3 SZC010 suppresses MDA-MB-453 cell proliferation in a dose- and time-dependent manner. MCF-10A and MDA-MB-453 cells were treated with various concentrations of SZC010 (5–40 μmol/L) for various time periods (12–72 h). (A) Line graphs showing the percentage of viable MDA-MB-453 cells following treatment with 5, 10, 15, 20, 30, and 40 μmol/L SZC010 for 12, 24, 48, and 72 h, as determined by the MTT assay. Data are expressed as the mean ± SEM of three independent experiments performed in triplicate. (B) Line graphs showing the percentage of viable MCF-10A cells following treatment with SZC010, as determined by the MTT assay. MTT, 3-(4,5-Dimethylthiazol-2-yl)-2,5-diphenyl tetrazolium bromide; SEM, standard error of the mean.

was performed to evaluate the apoptosis-related proteins. As shown in *Figure 4C,4D*, following treatment with 15 μmol/L SZC010 for 12, 24, and 48 h, a clear increase in the activation of cleaved caspase-3, cleaved caspase-9, and cleaved poly-ADP ribose polymerase (PARP) was observed, which was accompanied by a decrease in procaspase-3, procaspase-9, and PARP. It is known that the intrinsic apoptosis pathway, which involves B-cell lymphoma 2 (Bcl-2) family members, can activate the caspase cascade (24). Therefore, Bcl-XL, the Bcl-2-associated X protein (Bax), and key members of the Bcl-2 family were investigated. As shown in *Figure 4C,4D*, the expression of Bax was increased, while that of Bcl-XL and Bcl-2 decreased following SZC010 treatment. Moreover, it has been well established that cytochrome C (Cyto-c) binds to the apoptosis protease activation factor and forms an apoptosome, leading to apoptosis. As shown in *Figure 4C,4D*, treatment with 15 μmol/L SZC010 for 12 and 24 h increased the expression of Cyto-c, while treatment for 48 h decreased it. These results indicated that SZC010 induced caspase-dependent apoptosis through intrinsic pathways.

SZC010 induces G2/M phase arrest in MDA-MB-453 cells

A cell cycle analysis was performed to identify the possible mechanisms underlying the SZC010-induced reduction in the viability of MDA-MB-453 cells. As shown in *Figure 5A,5B* treatment with 15 μmol/L SZC010 for various periods resulted in a significant increase in the number of cells in the G2/M phase: 13.07%±3.45% at 12 h, 19.72%±1.72% at 24 h and 20.84%±4.79% at 48 h, as compared to the controls (3.84%±0.43%). Furthermore, the cyclin D1, D4, and B1 proteins, which regulate the G2/M phase of the cell cycle, were assessed by western blotting. As shown in *Figure 5C*, treatment with SZC010 decreased the protein levels of cyclin D1, D4, and B1 in a time-dependent manner. These results indicated that SZC010 induced G2/M phase arrest in MDA-MB-453 cells by cyclin proteins.

SZC014 suppresses nuclear factor-κB (NF-κB) activation in MDA-MB-453 cells

NF-κB belongs to a family of transcription factors that play a crucial role in tumor cell survival, angiogenesis, migration, etc. (25). In normal cells, NF-κB is cytoplasmically sequestered in a latent, inactive form that is bound to the inhibitor of κB (IκB) proteins. Cellular stimulation leads to the phosphorylation of IkBs and then releases the p65 subunit. Next, the p65 subunit translocates into the nucleus and binds to a specific consensus sequence of DNA (26). To determine whether the inhibitory effect of SZC010 in MDA-MB-453 cells is mediated by the suppression of NF-κB activation, the phosphorylation levels of IκBα and NF-κBp65 were measured by western blotting. As shown in *Figure 6A-6C*, a significant time-dependent inhibition in

© Chinese Clinical Oncology. All rights reserved.

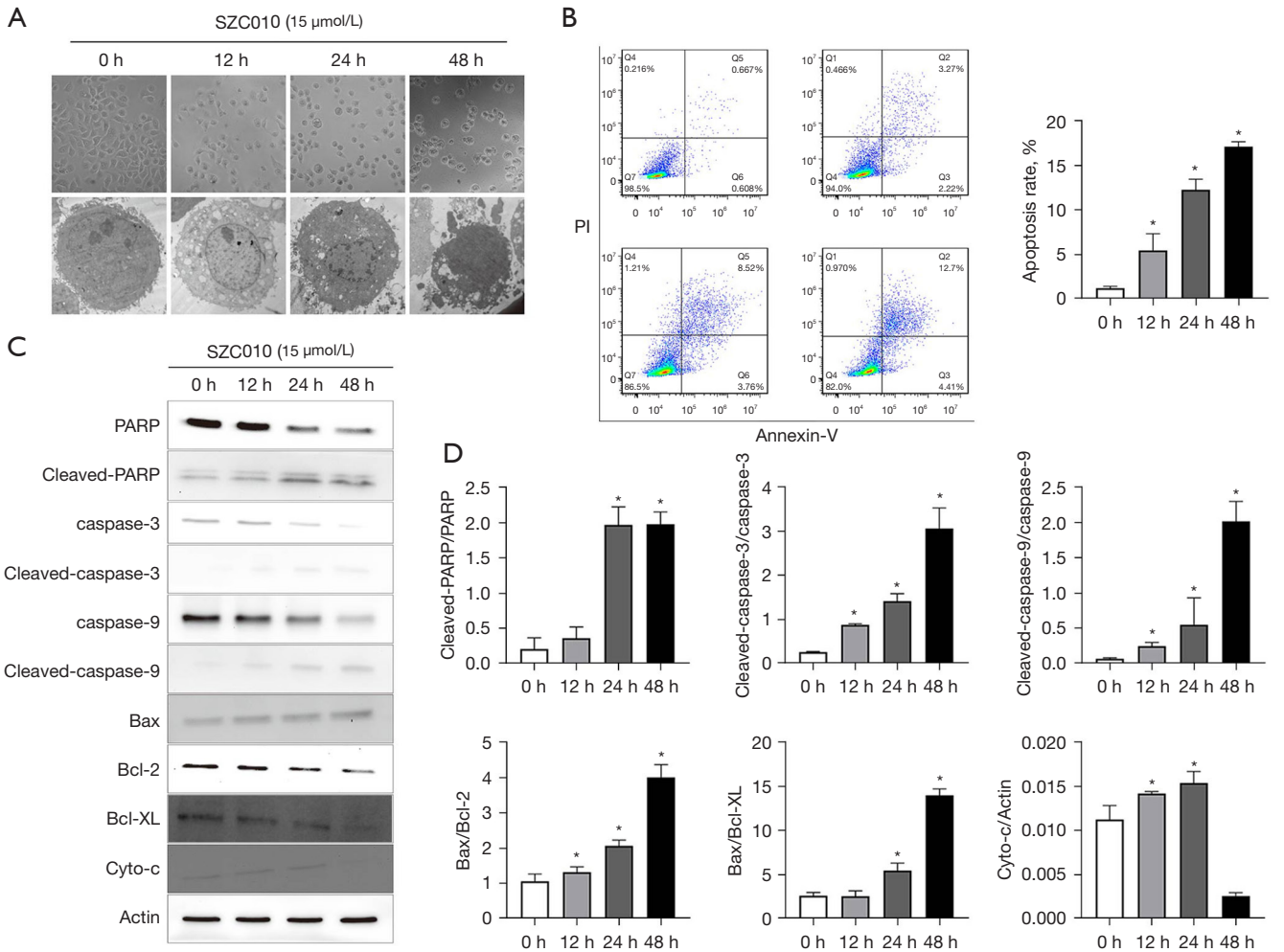

Figure 4 SZC010 induced apoptosis in MDA-MB-453 cells. MDA-MB-453 cells were treated with 15 μmol/L SZC010 for 12, 24, and 48 h. (A) Light (40×) and transmission electron microscopy (8,000×) results showing the apoptosis-related morphology and ultrastructure changes induced by SZC010. (B) Annexin V FITC/PI staining results showing SZC010-induced apoptosis. The apoptotic rate results are expressed as the mean ± SEM of three independent experiments performed in triplicate (n=3; *, P<0.05). (C) The expression levels of apoptosis-related proteins PARP, cleaved-PARP, caspase-3, cleaved-caspase-3, caspase-9, cleaved-caspase-9, Bax, Bcl-2, Bcl-XL, and Cyto-c were examined by western blotting. Actin was used as a loading control. The image is representative of three independent experiments yielding similar results. (D) The expression levels of apoptosis-related proteins, cleaved-PARP/PARP, cleaved-caspase-3/caspase-3, cleaved-caspase-9/caspase-9, Bax/Bcl-2, Bax/Bcl-XL, and Cyto-c/Actin, were quantified by Quantity One. Data are expressed as the mean ± SEM of three independent experiments performed in triplicate (n=3; *, P<0.05). PARP, poly-ADP ribose polymerase; Bax, Bcl-2-associated X protein; Bcl-2, B-cell lymphoma 2; Cyto-c, cytochrome c; FITC/PI, fluorescein isothiocyanate isomer I/propidium iodide; SEM, standard error of the mean.

the phosphorylation of IκBα and NF-κBp65 was observed following the treatment of MDA-MB-453 cells with SZC010. These results suggested that the inhibition of NF-κB activation was a mechanism through which SZC010 induced its anti-cancer activity.

SZC010 inhibits the PI3K/Akt/mTOR signaling pathway in MDA-MB-453 cells

To further elucidate the molecular mechanism of the anti-cancer activity of SZC010, the effect of SZC010 on the PI3K/Akt/mTOR signaling pathway was investigated.

© Chinese Clinical Oncology. All rights reserved.

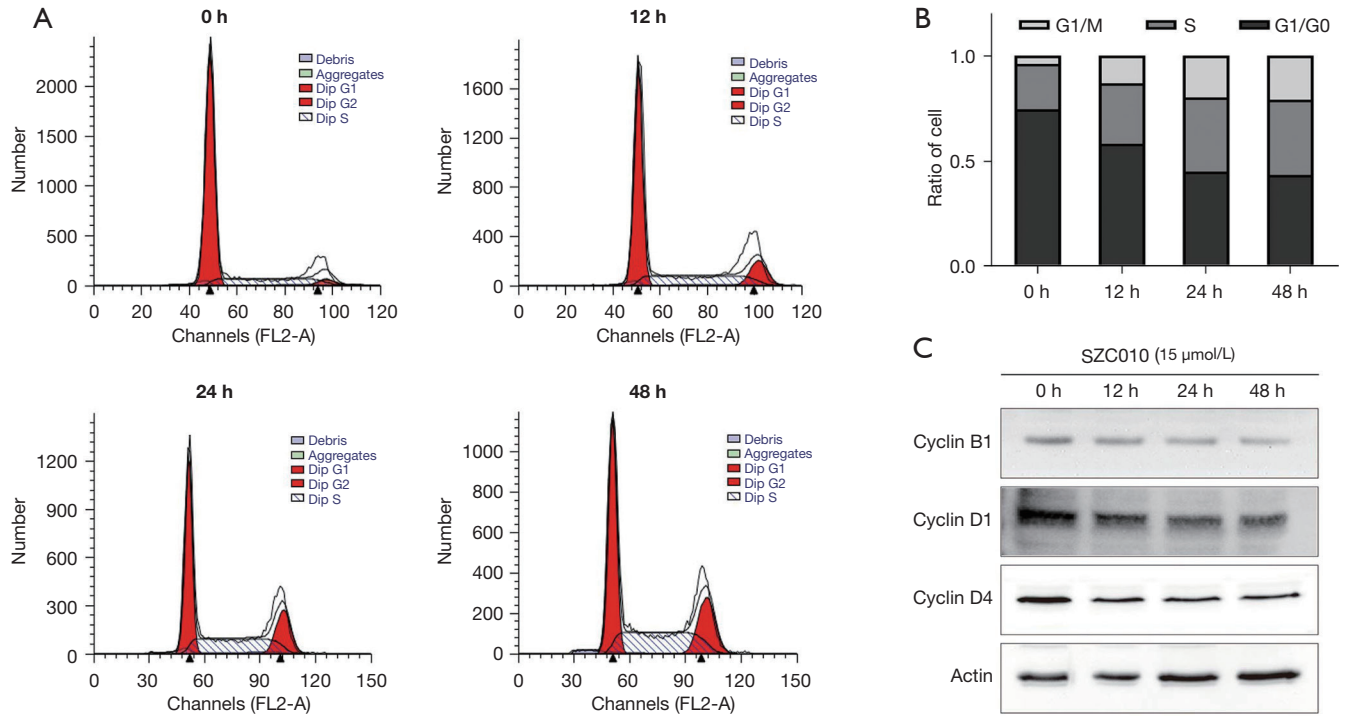

Figure 5 SZC010 induces G2/M phase arrest in MDA-MB-453 cells. MDA-MB-453 cells were treated with 15 μmol/L SZC010 for 12, 24, and 48 h. (A) Representative images showing the effect of SZC010 on cell cycle progression. G2/M phase arrest was observed in SZC010-treated MDA-MB-453 cells. (B) Histogram showing the cell cycle distribution quantification. (C) The expression levels of cell cycle-related proteins (cyclin D1, D4, and B1) were examined by western blotting. Actin was used as a loading control. The image is representative of three independent experiments yielding similar results.

PI3K (p110 and p85) and the phosphorylation levels of Akt, mTOR, and p70S6K were examined by western blotting in MDA-MB-453 cells. As shown in *Figure 7A*,*7B*, the treatment of MDA-MB-453 cells with SZC010 induced a time-dependent inhibition of the expression of the PI3K subunits, p85 and p110. In addition, SZC010 treatment downregulated the levels of phosphorylated Akt and mTOR in a time-dependent manner. SZC010 treatment also downregulated the phosphorylation of p70S6K, which is a downstream factor of mTOR. In addition, SZC010 could repress the expression of PI3K (p110 and p85), leading to the suppression of Akt and mTOR phosphorylation, which in turn resulted in the suppression of p70S6K phosphorylation. The present results revealed that the inhibition of PI3K/Akt/mTOR signaling was a mechanism through which SZC010 induced its anti-cancer activity.

SZC010 suppresses tumor growth in tumor-bearing mice

To confirm the antitumor effect of SZC010 *in vivo*, BALB/c mice with an intact immune system were implanted with MDA-MB-453 cells in the armpits. We separated the mice into two groups: (I) vehicle i.p.; (II) SZC010 (10 mg/kg SZC010, i.p., once every 2 days) groups. The representative changes of tumors were displayed in *Figure 8A-8D*, showing a significantly lower tumor size in the SZC010 group than that in the vehicle group. No significant differences were found in the mean body weights of tumor-bearing mice between the SZC010 and vehicle groups, indicating low toxicity of SZC010 *in vivo*. The average tumor weights were 0.564±0.118 and 0.412±0.071 g in the vehicle and SZC010 groups, respectively, in the nude mouse model (*Figure 8E*). Moreover, western blot analysis of the tumor tissues revealed that the expressions of the PI3K/Akt/mTOR

© Chinese Clinical Oncology. All rights reserved.

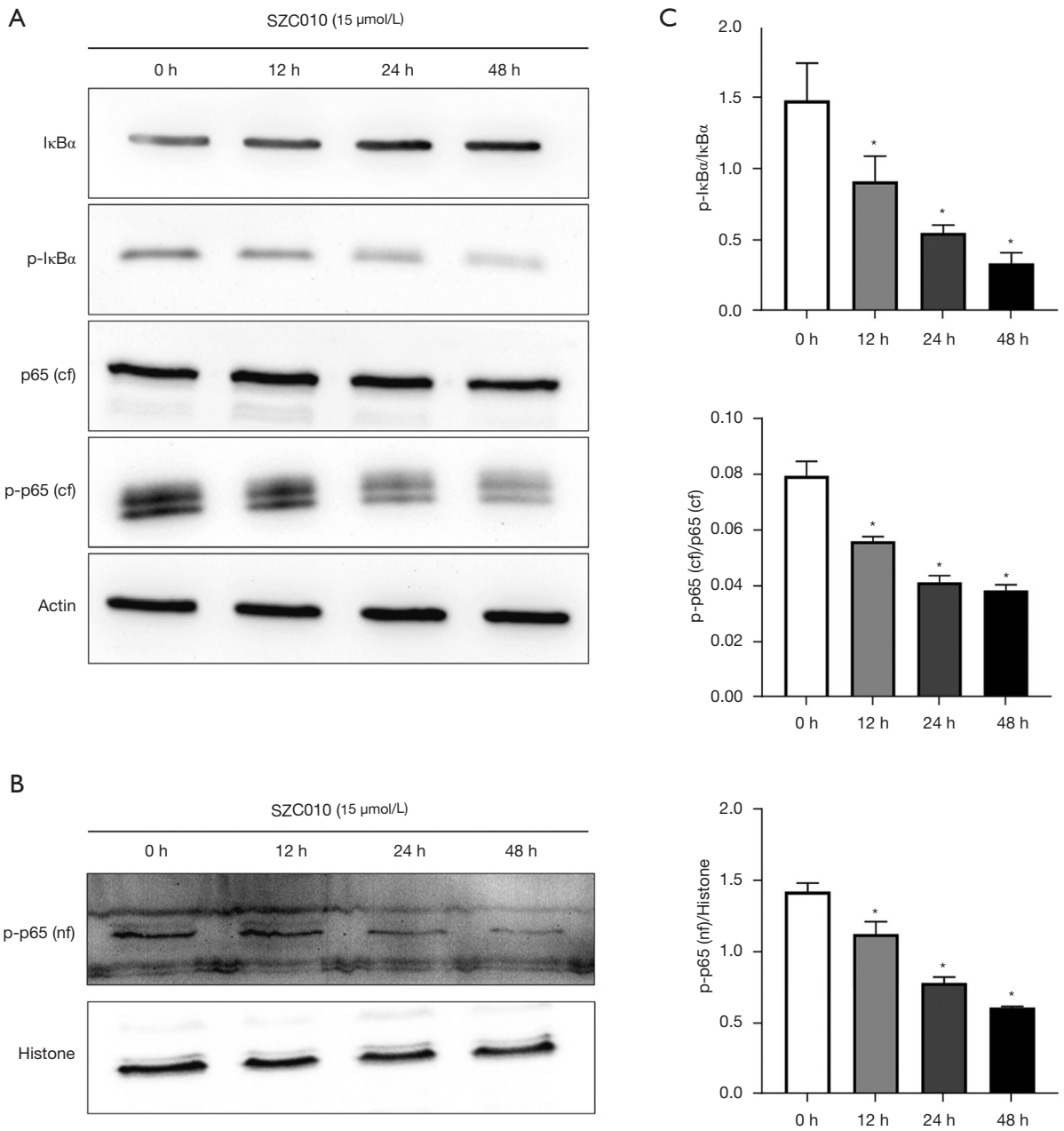

Figure 6 SZC014 suppresses NF-κB activation in MDA-MB-453 cells. MDA-MB-453 cells were treated with 15 μmol/L SZC010 for 12, 24, and 48 h. (A) The expression levels of proteins in the cytoplasm involved in NF-κB activation (IκB, p-IκB, p65, and p-p65) were examined by western blotting. Actin was used as a loading control. The image is representative of three independent experiments yielding similar results. (B) The expression level of p-p65 in the nucleus was examined by western blotting. Histone was used as a loading control. The image is representative of three independent experiments yielding similar results. (C) The expression levels of NF-κB signaling pathway proteins [p-IκBα/IκBα, p-p65(cf)/p65(cf), and p-p65(nf)/Histone] were quantified by Quantity One. Data are expressed as the mean ± SEM of three independent experiments performed in triplicate (n=3; *, P<0.05). NF-κB, nuclear factor-κB; IκB, inhibitor of κB; SEM, standard error of the mean.

© Chinese Clinical Oncology. All rights reserved.

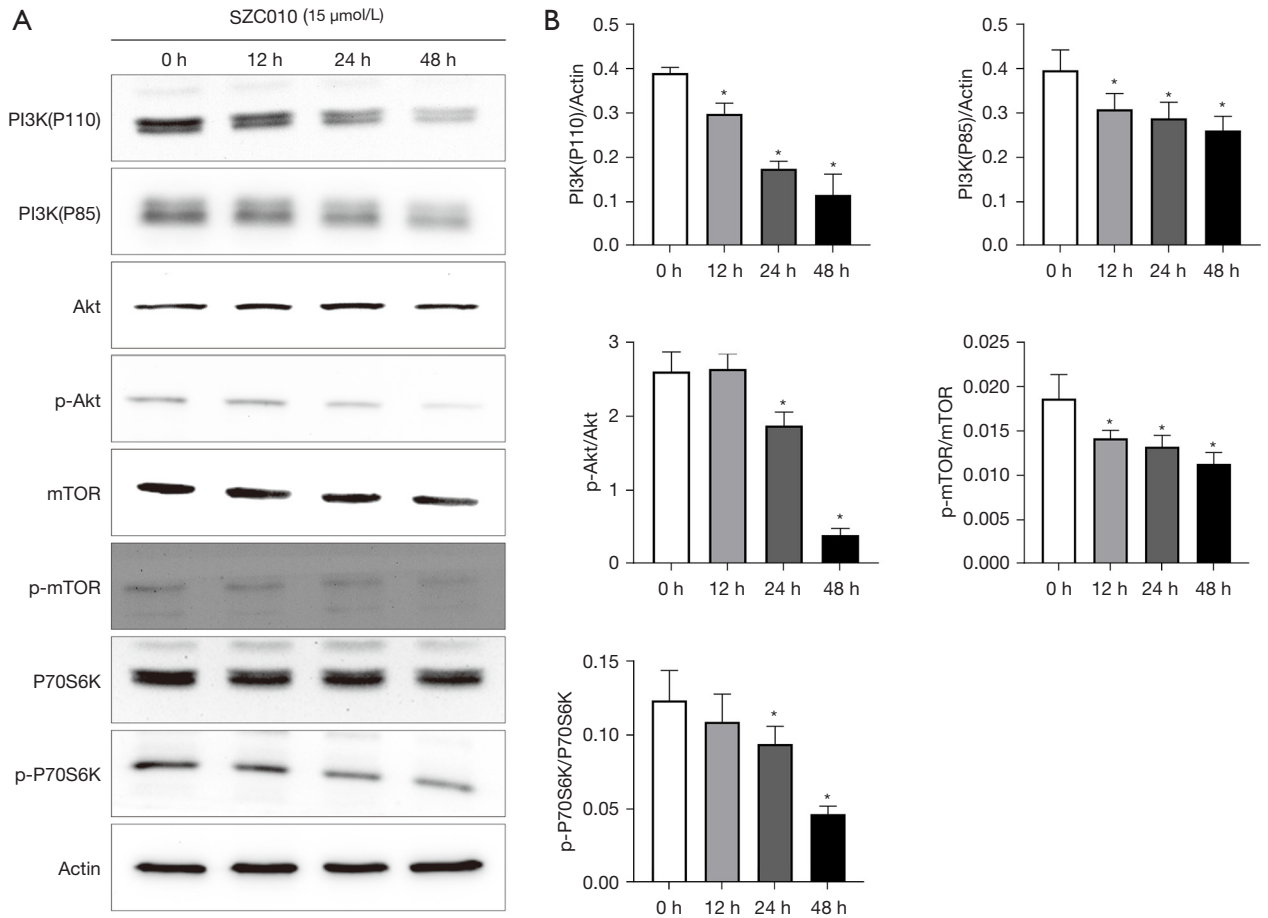

Figure 7 SZC010 inhibits the PI3K/Akt/mTOR signaling pathway in MDA-MB-453 cells. MDA-MB-453 cells were treated with 15 μmol/L SZC010 for 12, 24, and 48 h. (A) The expression levels of PI3K/Akt/mTOR signaling pathway proteins [PI3K(P110), PI3K(P85), Akt, p-Akt, mTOR, p-mTOR, P70S6K, and p-P70S6K] were examined by western blotting. Actin was used as a loading control. The image is representative of three independent experiments yielding similar results. (B) The expression levels of PI3K/Akt/mTOR signaling pathway proteins [PI3K(P110)/Actin, PI3K(P85)/Actin, p-Akt/Akt, p-mTOR/mTOR, and p-P70S6K/P70S6K] were quantified by Quantity One. Data are expressed as the mean ± SEM of three independent experiments performed in triplicate (n=3; *, P<0.05). SEM, standard error of the mean.

and NF-κB signaling pathway were reduced by SZC010 treatment, as compared to the vehicle group (*Figure 8F*).

Discussion

OA (also known as 3β-hydroxyolean-12-en-28-oic acid), which belongs to the Oleaceae family, is a bioactive pentacyclic triterpenoid that can be isolated from >1,600 plant species (27-29). OA has been shown to exert antitumor activities against numerous neoplasms, including hepatocellular cancer, hematological malignancies, lung cancer, ovarian cancer, pancreatic cancer, skin cancer, glioblastoma, and breast cancer. A study has confirmed that OA has relatively weak antitumor activity against breast cancer due to poor water solubility (30); structural modifications may therefore be a feasible strategy to improve the anticancer activity of OA by enhancing its water solubility. Huang *et al.* (31) synthesized a 3-oxo-OA via Jones oxidation reactions and improved its antitumor activity in melanoma *in vitro* and *in vivo*.

Based on 3-oxo-OA, seven nitrogen-containing OA derivatives were synthesized by the Mannich and fused heterocycle reactions. In the present study, the efficacy of these compounds was evaluated against different cancer

© Chinese Clinical Oncology. All rights reserved.

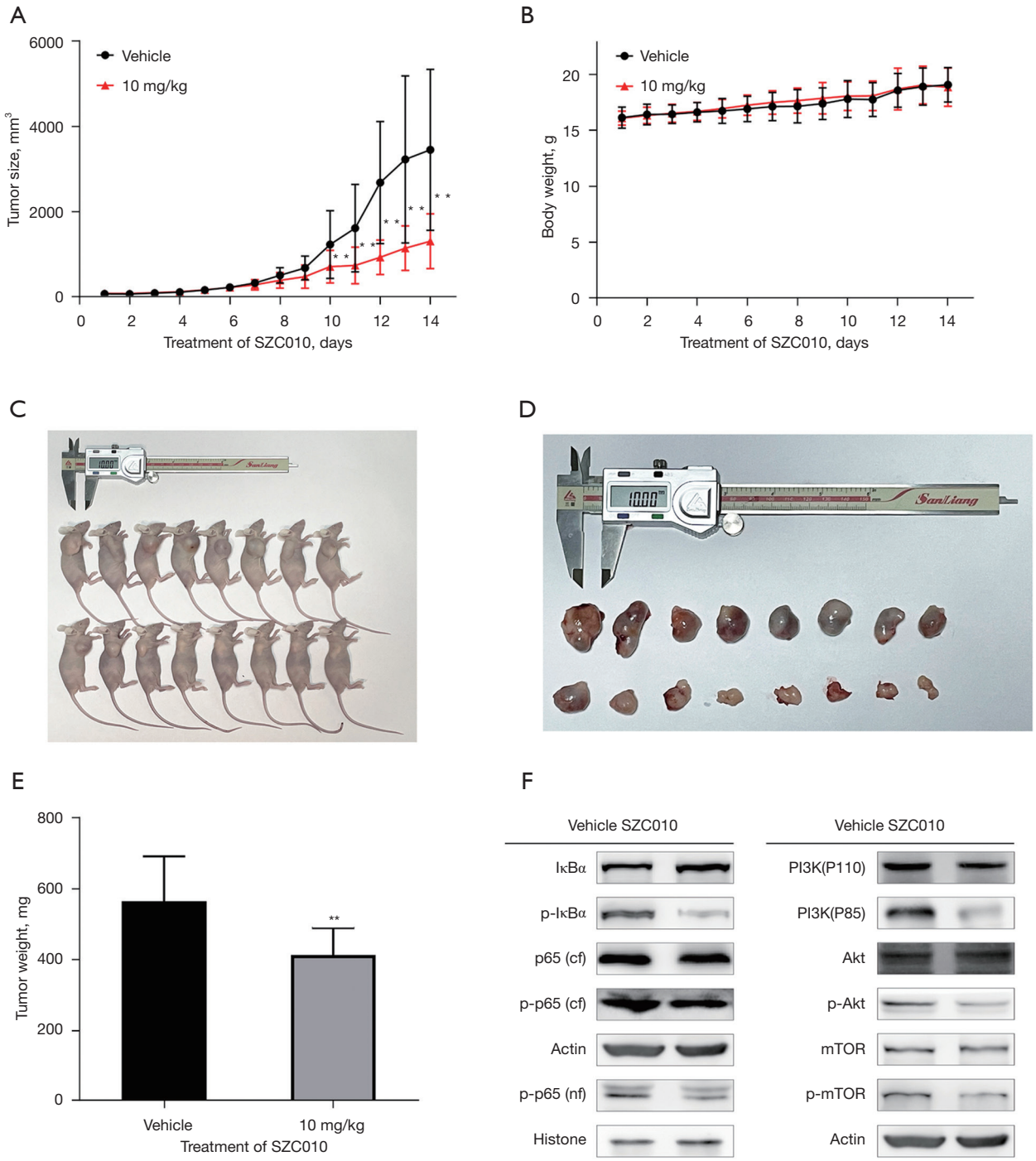

Figure 8 SZC010 inhibited tumor growth *in vivo*. (A) The growth curves of tumors at the indicated days following SZC010 treatment (**, P<0.01). (B) No significant difference was found in the body weights of tumor-bearing mice between the treatment and vehicle groups. (C) The mice were executed and photographed after a 2-week treatment. (D) The tumors were excised from mice and photographed after a 2-week treatment. (E) The average tumor weight of the SZC010 treatment group was significantly decreased compared with that of the vehicle group. Data are expressed as the mean ± SEM (**, P<0.01). (F) Proteins were extracted from the tumors, and western blot was used to detect their expressions. SEM, standard error of the mean.

© Chinese Clinical Oncology. All rights reserved.

cell lines including gastric, pancreatic, and lung cancer cell lines. Generally, these seven nitrogen-containing OA derivatives were more cytotoxic than OA, and the Mannich derivatives were more effective than the fused heterocycle derivatives. As expected, our findings revealed that all of the OA derivatives were more effective than OA in three breast cancer cell lines. Notably, the Mannich base derivatives exhibited markedly better antiproliferative activity than the fused heterocycle derivatives in MCF-7 and MDA-MB-231 cell lines, while the fused heterocycle derivatives were more effective in the MDA-MB-453 cell lines, indicating that the fused heterocycle derivatives, particularly SZC010, were highly selective toward MDA-MB-453 cells. Furthermore, in the xenograft model, we also found a significantly lower tumor size and weight in the SZC010 group compared to the vehicle group.

Apoptosis plays an important role in the destruction of undesired cells under pathological or aging conditions (32). However, apoptotic signals are inhibited in cancer cells, indicating that targeting apoptotic signals is an attractive cancer therapeutic strategy (33). By morphology/ultrastructure and flow cytometry, we found that SZC010 effectively inhibited the growth of MDA-MB-453 cells by inducing apoptosis. It is known that the intrinsic mitochondrial and extrinsic pathways could be the mechanisms triggering apoptosis (34). For the intrinsic mitochondrial pathway, the proapoptotic Bax protein tightly binds to the anti-apoptotic proteins, Bcl-2/Bcl-XL, residing on the outer mitochondrial membrane. When released from Bcl-2, an outer mitochondrial membrane oligomeric channel is formed by Bax, which facilitates Cyto-c release to promote cell death (35). The present result demonstrated that SZC010 increased the protein expression of Bax and inhibited that of Bcl-2/Bcl-XL, thus increasing the Cyto-c release and triggering the cleavage of caspases 9 and 3; this indicated that SZC010 induced apoptosis through the mitochondria-mediated intrinsic pathway.

It has been established that controlling the cell cycle is an effective way to inhibit cancer progression, as regulators of the cell cycle are frequently deregulated in most neoplasms (36). Through cell cycle analysis, the present data showed that SZC010 treatment induced G2/M phase arrest in MDA-MB-453 cells and decreased the expression level of cyclin D1, D4, and B1.

Breast cancer is a heterogeneous disease that is clinically subdivided into HR+, HER2^{+}, and TNBC. Undoubtedly, the strategies that target HER2 are the most successful for cancer therapeutics in the clinic. HER2 amplification/overexpression accounts for 25–30% of all breast cancer cases and is associated with the aggressiveness of carcinoma growth and resistance to treatment, leading to recurrent disease progression or poor prognosis (37-39). HER2 is a member of the epidermal growth factor receptor (EGFR/HER) family comprising EGFR (HER1), HER2, HER3, and HER4 (40). The homo- or hetero-dimerization of these receptors induces the transphosphorylation of specific tyrosine residues in their intracellular domain(s), resulting in the initiation of downstream signaling pathways including the PI3K/Akt/mTOR signaling pathway (41). HER2 can indirectly couple to the p85 regulatory subunit of PI3K by forming heterodimers with HER3 or recruiting adapters (GRB2-GAB1 or GAB2), resulting in the activation of PI3K (42,43).

Following the activation of PI3K, Akt is subsequently phosphorylated and activated. The phosphorylated form of Akt indirectly activates mTOR, which is usually coupled with other proteins in a complex known as mTORC1 (44). In the mTORC1, mTOR phosphorylates p70S6K (70 kDa ribosomal protein S6 kinase), leading to increased translation and synthesis of cell cycle-regulating and apoptosis-related proteins (45). In addition, the activated form of Akt also promotes the malignant transformation of the inhibitory kB kinases. These activated kinases then phosphorylate the IkBs and cleave to release the p65 subunit, which translocates into the nucleus and binds to a specific consensus sequence of DNA; the latter is involved in multiple biological processes, including cell cycle control and apoptosis (46). These results demonstrated that SZC010 treatment in MDA-MB-453 cells resulted in the inhibition of the PI3K/Akt/mTOR signaling pathway and NF-κB activation.

In the present study, we observed that SZC010 inhibited NF-κB activation and the PI3K/Akt/mTOR signaling pathway, thereby inducing apoptosis and G2/M phase arrest in HER2-overexpressed MDA-MB-453 cells. Our previous studies showed that OA and its derivatives can suppress NF-κB activation in numerous types of cancer (47,48). The present results identified that SZC010 induced-apoptosis and inhibition of NF-κB activation are mediated via PI3K/Akt/mTOR signaling pathway inhibition. Thus, we hypothesized that the higher potency anticancer activity of SZC010 in HER2-overexpressed MDA-MB-453 cells was associated with its high selectivity towards the PI3K/Akt/mTOR signaling pathway. Moreover, the present research further established that the PI3K/Akt/mTOR signaling pathway is associated with HER2-directed resistance to

© Chinese Clinical Oncology. All rights reserved.

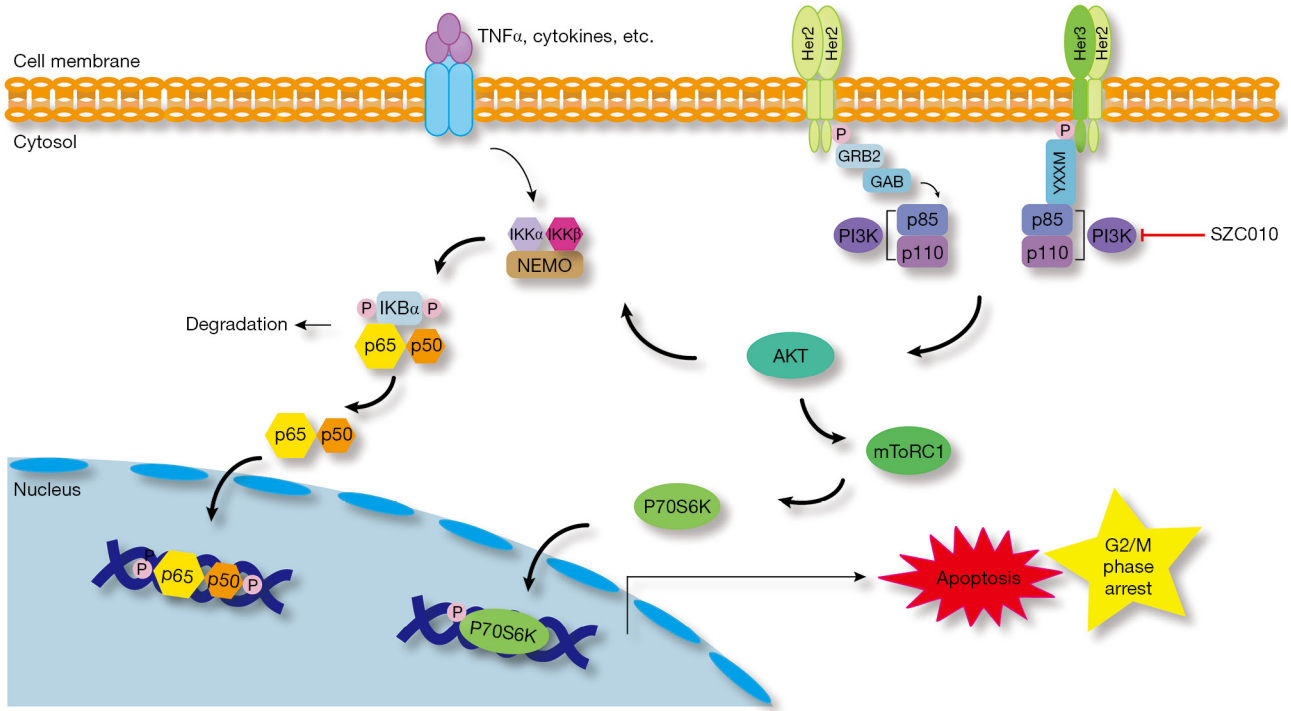

Figure 9 Proposed model for SZC010-induced cell death in the MDA-MB-453 cell line.

clinical treatment (49). Our next study will also focus on the mechanism underlying the resistance of SZC010 to anti-HER2 therapies.

Conclusions

In conclusion, seven nitrogen-containing OA derivatives were synthesized via the Mannich and fused heterocycle reactions. All OA derivatives were more effective than OA in the three types of breast cancer cell lines (MCF-7, MDA-MB-231, and MDA-MB-453). Among these seven OA derivatives, SZC010 exhibited the most potent cytotoxic activity in the MDA-MB-453 cell line and xenograft model. It was also observed that SZC010 treatment induced a dose- and time-dependent inhibition of MDA-MB-453 cell growth. Furthermore, we also observed that SZC010 induced apoptosis and G2/M phase arrest via PI3K/Akt/NF-κB signaling pathway inhibition (*Figure 9*). The present data indicated that the novel OA derivative, SZC010, has great potential in cancer therapy.

Acknowledgments

This work was also presented in the CCTB 2021 as a poster.

Funding: This work was partly supported by grants from the Natural Science Foundation of Liaoning Province (No. 20180551215), the Key R&D Guidance Plan of Liaoning Province (No. 2019JH8/10300020), the Science and Technology Plan Project of Liaoning Province (No. 2013225585), the Key Program of China Association for the Promotion of Health (No. CHPF-RX080301), and the Fundamental Research Funds for the Central Universities (No. LD2023024).

Footnote

Reporting Checklist: The authors have completed the MDAR and ARRIVE reporting checklists. Available at https://cco.amegroups.com/article/view/10.21037/cco-24-10/rc

Data Sharing Statement: Available at https://cco.amegroups.com/article/view/10.21037/cco-24-10/dss

Peer Review File: Available at https://cco.amegroups.com/article/view/10.21037/cco-24-10/prf

Conflicts of Interest: All authors have completed the ICMJE

© Chinese Clinical Oncology. All rights reserved.

uniform disclosure form (available at https://cco.amegroups.com/article/view/10.21037/cco-24-10/coif). The authors have no conflicts of interest to declare.

Ethical Statement: The authors are accountable for all aspects of the work in ensuring that questions related to the accuracy or integrity of any part of the work are appropriately investigated and resolved. Animal experiments were performed under a project license (No. CMU2023040) granted by Animal Ethics Committee board of China Medical University, in compliance with China Medical University's guidelines for the care and use of animals.

Open Access Statement: This is an Open Access article distributed in accordance with the Creative Commons Attribution-NonCommercial-NoDerivs 4.0 International License (CC BY-NC-ND 4.0), which permits the non-commercial replication and distribution of the article with the strict proviso that no changes or edits are made and the original work is properly cited (including links to both the formal publication through the relevant DOI and the license). See: https://creativecommons.org/licenses/by-nc-nd/4.0/.

References

1. Giaquinto AN, Sung H, Miller KD, et al. Breast Cancer Statistics, 2022. CA Cancer J Clin 2022;72:524-41.
2. Fillon M. Breast cancer recurrence risk can remain for 10 to 32 years. CA Cancer J Clin 2022;72:197-9.
3. Spring LM, Wander SA, Andre F, et al. Cyclin-dependent kinase 4 and 6 inhibitors for hormone receptor-positive breast cancer: past, present, and future. Lancet 2020;395:817-27.
4. Savioli F, Edwards J, McMillan D, et al. The effect of postoperative complications on survival and recurrence after surgery for breast cancer: A systematic review and meta-analysis. Crit Rev Oncol Hematol 2020;155:103075.
5. Montero A, Ciérvide R, García-Aranda M, et al. Postmastectomy radiation therapy in early breast cancer: Utility or futility? Crit Rev Oncol Hematol 2020;147:102887.
6. Goutsouliak K, Veeraraghavan J, Sethunath V, et al. Towards personalized treatment for early stage HER2-positive breast cancer. Nat Rev Clin Oncol 2020;17:233-50.
7. Hanker AB, Sudhan DR, Arteaga CL. Overcoming Endocrine Resistance in Breast Cancer. Cancer Cell 2020;37:496-513.
8. Fares JE, El Tomb P, Khalil LE, et al. Metronomic chemotherapy for patients with metastatic breast cancer: Review of effectiveness and potential use during pandemics. Cancer Treat Rev 2020;89:102066.
9. Egger SJ, Chan MMK, Luo Q, et al. Platinum-containing regimens for triple-negative metastatic breast cancer. Cochrane Database Syst Rev 2020;10:CD013750.
10. McGee SF, Clemons M, Savard MF. Evolving Role of Risk Tailored Therapy in Early Stage HER2-Positive Breast Cancer: A Canadian Perspective. Curr Oncol 2022;29:4125-37.
11. Choong GM, Cullen GD, O'Sullivan CC. Evolving standards of care and new challenges in the management of HER2-positive breast cancer. CA Cancer J Clin 2020;70:355-74.
12. Gill J, Yendamuri K, Chatterjee U, et al. Racial/ethnic differences in 21-gene recurrence score and survival among patients with estrogen receptor-positive breast cancer. BMC Cancer 2024;24:461.
13. Wu J, Fan D, Shao Z, et al. CACA Guidelines for Holistic Integrative Management of Breast Cancer. Holist Integr Oncol 2022;1:7.
14. Xue JX, Zhu ZY, Bian WH, et al. The Traditional Chinese Medicine Kangai Injection as an Adjuvant Method in Combination with Chemotherapy for the Treatment of Breast Cancer in Chinese Patients: A Meta-Analysis. Evid Based Complement Alternat Med 2018;2018:6305645.
15. Yang H, Deng M, Jia H, et al. A review of structural modification and biological activities of oleanolic acid. Chin J Nat Med 2024;22:15-30.
16. Kamran S, Sinniah A, Abdulghani MAM, et al. Therapeutic Potential of Certain Terpenoids as Anticancer Agents: A Scoping Review. Cancers (Basel) 2022;14:1100.
17. Fontana G, Badalamenti N, Bruno M, et al. Synthesis, In Vitro and In Silico Analysis of New Oleanolic Acid and Lupeol Derivatives against Leukemia Cell Lines: Involvement of the NF-κB Pathway. Int J Mol Sci 2022;23:6594.
18. Shukla VN, Vikas, Mehata AK, et al. EGFR targeted albumin nanoparticles of oleanolic acid: In silico screening of nanocarrier, cytotoxicity and pharmacokinetics for lung cancer therapy. Int J Biol Macromol 2023;246:125719.
19. Zeng Z, Yu J, Jiang Z, et al. Oleanolic Acid (OA) Targeting UNC5B Inhibits Proliferation and EMT of Ovarian Cancer Cell and Increases Chemotherapy Sensitivity of Niraparib. J Oncol 2022;2022:5887671.
20. Wei J, Liu M, Liu H, et al. Oleanolic acid arrests cell cycle and induces apoptosis via ROS-mediated mitochondrial depolarization and lysosomal membrane permeabilization

© Chinese Clinical Oncology. All rights reserved.

in human pancreatic cancer cells. J Appl Toxicol 2013;33:756-65.
21. Hata K, Hori K, Takahashi S. Differentiation- and apoptosis-inducing activities by pentacyclic triterpenes on a mouse melanoma cell line. J Nat Prod 2002;65:645-8.
22. Martín R, Carvalho-Tavares J, Ibeas E, et al. Acidic triterpenes compromise growth and survival of astrocytoma cell lines by regulating reactive oxygen species accumulation. Cancer Res 2007;67:3741-51.
23. Tang ZY, Li Y, Tang YT, et al. Anticancer activity of oleanolic acid and its derivatives: Recent advances in evidence, target profiling and mechanisms of action. Biomed Pharmacother 2022;145:112397.
24. Iksen, Witayateeraporn W, Hardianti B, et al. Comprehensive review of Bcl-2 family proteins in cancer apoptosis: Therapeutic strategies and promising updates of natural bioactive compounds and small molecules. Phytother Res 2024;38:2249-75.
25. Van Bockstal MR, Agahozo MC, van Marion R, et al. Somatic mutations and copy number variations in breast cancers with heterogeneous HER2 amplification. Mol Oncol 2020;14:671-85.
26. Kubatka P, Koklesova L, Mazurakova A, et al. Cell plasticity modulation by flavonoids in resistant breast carcinoma targeting the nuclear factor kappa B signaling. Cancer Metastasis Rev 2024;43:87-113.
27. Li Y, Wang J, Li L, et al. Natural products of pentacyclic triterpenoids: from discovery to heterologous biosynthesis. Nat Prod Rep 2023;40:1303-53.
28. Vite MH, Sonawane MI, Vayal PM. Oleanolic acid as a potential drug molecule: A review. World J Adv Res Rev 2023;17:249-54.
29. Chen C, Ai Q, Shi A, et al. Oleanolic acid and ursolic acid: therapeutic potential in neurodegenerative diseases, neuropsychiatric diseases and other brain disorders. Nutr Neurosci 2023;26:414-28.
30. Gao CX, Tang CH, Wu TJ, et al. Anticancer activity of oleanolic acid and its derivatives modified at A-ring and C-28 position. J Asian Nat Prod Res 2023;25:581-94.
31. Huang D, Ding Y, Li Y, et al. Anti-tumor activity of a 3-oxo derivative of oleanolic acid. Cancer Lett 2006;233:289-96.
32. Ahmed KR, Rahman MM, Islam MN, et al. Antioxidants activities of phytochemicals perspective modulation of autophagy and apoptosis to treating cancer. Biomed Pharmacother 2024;174:116497.
33. Hanahan D. Hallmarks of Cancer: New Dimensions. Cancer Discov 2022;12:31-46.
34. Sun G. Death and survival from executioner caspase activation. Semin Cell Dev Biol 2024;156:66-73.
35. Allani M, Akhilesh, Tiwari V. Caspase-driven cancer therapies: Navigating the bridge between lab discoveries and clinical applications. Cell Biochem Funct 2024;42:e3944.
36. Fuentes-Antrás J, Bedard PL, Cescon DW. Seize the engine: Emerging cell cycle targets in breast cancer. Clin Transl Med 2024;14:e1544.
37. Fernandes CL, Silva DJ, Mesquita A. Novel HER-2 Targeted Therapies in Breast Cancer. Cancers (Basel) 2023;16:87.
38. Uribe ML, Marrocco I, Yarden Y. EGFR in Cancer: Signaling Mechanisms, Drugs, and Acquired Resistance. Cancers (Basel) 2021;13:2748.
39. Sánchez-Lorenzo L, Bachiller A, Gea C, et al. Current Management and Future Perspectives in Metastatic HER2-Positive Breast Cancer. Semin Oncol Nurs 2024;40:151554.
40. Wu X, Huang S, He W, et al. Emerging insights into mechanisms of trastuzumab resistance in HER2-positive cancers. Int Immunopharmacol 2023;122:110602.
41. Premji SK, O'Sullivan CC. Standard-of-Care Treatment for HER2+ Metastatic Breast Cancer and Emerging Therapeutic Options. Breast Cancer (Auckl) 2024;18:11782234241234418.
42. Robert M, Frenel JS, Bourbouloux E, et al. Pertuzumab for the treatment of breast cancer. Expert Rev Anticancer Ther 2020;20:85-95.
43. Khorasani ABS, Hafezi N, Sanaei MJ, et al. The PI3K/AKT/mTOR signaling pathway in breast cancer: Review of clinical trials and latest advances. Cell Biochem Funct 2024;42:e3998.
44. Occhiuzzi MA, Lico G, Ioele G, et al. Recent advances in PI3K/PKB/mTOR inhibitors as new anticancer agents. Eur J Med Chem 2023;246:114971.
45. Javarsiani MH, Javanmard SH, Sajedianfard J. Expression of mTOR/70S6K signaling pathway in melanoma cancer cell and the effects of dacarbazine and metformin. Curr Cancer Ther Rev 2022;18:118-22.
46. Das R, Mehta DK, Dhanawat M. Medicinal Plants in Cancer Treatment: Contribution of Nuclear Factor-Kappa B (NF-kB) Inhibitors. Mini Rev Med Chem 2022;22:1938-62.
47. Rui LX, Shu SY, Jun WJ, et al. The dual induction of apoptosis and autophagy by SZC014, a synthetic oleanolic acid derivative, in gastric cancer cells via NF-κB pathway. Tumour Biol 2016;37:5133-44.
48. Song Y, Gao L, Tang Z, et al. Anticancer effect of

© Chinese Clinical Oncology. All rights reserved.

SZC015 on pancreatic cancer via mitochondria-dependent apoptosis and the constitutive suppression of activated nuclear factor κB and STAT3 in vitro and in vivo. J Cell Physiol 2018;234:777-88.
49. Fiascarelli A, Merlino G, Capano S, et al. Antitumor activity of the PI3K δ-sparing inhibitor MEN1611 in PIK3CA mutated, trastuzumab-resistant HER2 + breast cancer. Breast Cancer Res Treat 2023;199:13-23.

(English Language Editor: A. Kassem)

Cite this article as: Jiang J, Li X, Xu H, Ma Y, Fu M, Guo X, Sun T, Zheng X. SZC010 suppresses breast cancer development by regulating the PI3K/Akt/NF-κB signaling pathway. Chin Clin Oncol 2024;13(3):34. doi: 10.21037/cco-24-10

© Chinese Clinical Oncology. All rights reserved.